# Simulation of Current Collector Corrosion Effects on the Efficiency of Molten Carbonate Fuel Cells

I. Sgura[1], F. Zarcone[2] and B. Bozzini[*,2]
[1]Dipartimento di Matematica, Università del Salento, via per Arnesano., 73100, Lecce (I)
[2]Brindisi Fuel Cell Durability Laboratory, Facoltà di Ingegneria Industriale, Università del Salento, Cittadella della Ricerca S.S. 7 Brindisi-Taranto km 7+300 - 72100 Brindisi (I)
*Corresponding author: benedetto.bozzini@unile.it

**Abstract:** Corrosion and contact ohmic resistance of the stainless steel current collectors in molten carbonates is one of the greater obstacles to the widespread application of molten carbonate fuel cells (MCFC). This paper consists of two parts. In the first part, we simulate the variation of material parameters values, accounting for the impact of the corrosion of metallic current collectors on the performance of the porous cathode. In the second part we couple a thermal equation to the model and introduce appropriate dependencies upon the temperature on model parameters. The effects of the variation of single and combined material parameters on the current efficiency was ranked by a 2-level DOE analysis: catalyst poisoning resulted the single quantity most critically affecting cathodic efficiency.

**Keywords:** MCFC, cathode current collectors, corrosion, agglomerate model.

## 1. Introduction

One of the most critical barriers to the widespread commercial application of Molten Carbonate Fuel Cells (MCFCs) - and fuel cells in general - is durability. Corrosion of metallic components - and in particular of current collectors - is the single most critical issue in terms of impact on durability due to the growth of thick oxide scales with poor electrical conductivity, causing notable cell voltage loss [1, 2]. Voltage decay is related to loss of electrolyte by reaction with the growing oxide scale and to the increase of the ohmic resistance at the point of contact between the corroded current collector and the cathode. Furthermore, the necessity of using metals in the construction of MCFCs, in comparison with PEMFCs and SOFCs, calls for special research and development efforts in tackling environmental stability problems of metallic components. So far, the focus has been essentially on: (i) the assessment of the behavior of commercially available materials - mainly stainless steel grades - in simulated or real MCFC conditions, (ii) the development and testing of innovative corrosion-resistant alloys or protective coatings and (iii) materials science research into the elucidation of corrosion mechanisms.

This group has recently set up a laboratory aimed at combining experimental results of material performance with mathematical modeling at the system level for room- and high-pressure PEMFCs, MCFCs (the relevant facility is depicted in Fig. 1) and SOFCs. To the best of the authors' knowledge, no reports are available on the mathematical modeling of corrosion-related durability issues for MCFCs. The authors have recently attacked cognate problems in PEMFCs with this methodology [3] and are proposing their first results relevant to MCFCs in this report.

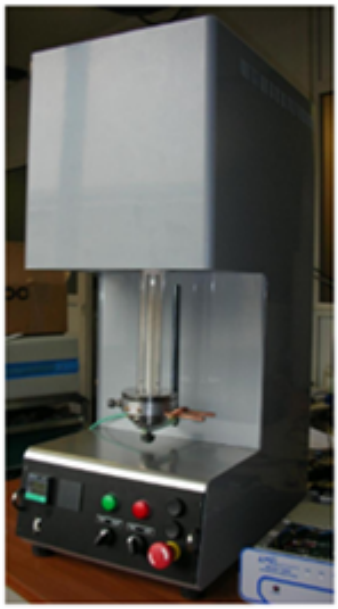

**Figure 1**. MCFC corrosion test ring.

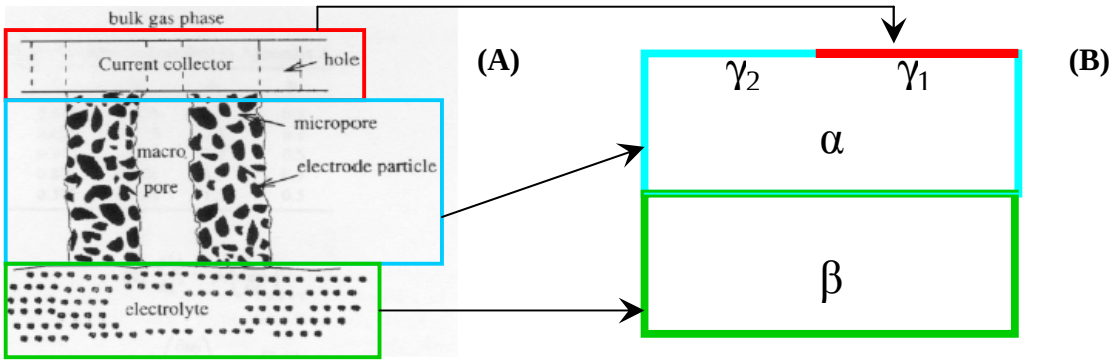


**Figure 2.** Geometric representation of a porous electrode in the agglomerate model (A) and the corresponding domains for the mathematical model (B), where α is the porous cathode, β is the free electrolyte, $\gamma_1$ models the solid metallic part of the current collector, and $\gamma_2$ simulates the holes bored in the current collector.

## 2. The Agglomerate Model

In [4, 5] a model was developed in order to investigate the effect of various parameters on the performance of the MCFC, based on the homogenization of the porous cathodes.Fig. 2 depicts the concept of the agglomerate model, based on the assumption that the electrode pores can be divided into two groups: micro-pores flooded with electrolyte and macro-pores, that act as gas channels. The micro porous agglomerates are assumed to be pseudo-homogeneous and are usually modeled as cylinders.

Making the agglomerate model assumption of [4, 5], the balances for ionic and electric currents in the cathode (α in Fig. 2B) and in the electrolyte (β in Fig. 2B) domains are written by combining Ohm's law for current transport and Kirchhoff's law for current conservation:

$$\left.\begin{aligned}\nabla i_{a,b} + S_{a,b} &= 0\\ i_{a,b} &= \kappa_{a,b}\cdot\nabla\phi_{a,b}\end{aligned}\right\} \rightarrow \kappa_{a,b}\cdot\nabla^2\phi_{a,b} + S_{a,b} = 0$$

where *a* denotes the type of charged species (ion *I* or electron *e*); *b* the relevant domain (cathode *c* or electrolyte *el*); $i_{a,b}$ are current densities; $\phi_{a,b}$ are phase electrical potentials and $\kappa_{a,b}$ are electrical conductivities. The source terms are obtained by linearizing the Butler-Volmer expression:

$$S_{a,b} = \left\{i_{a,b}^{(0)}\left([O_2]\right)\right\}\cdot\left\{\exp\left[\frac{\eta}{B_{a,b}^{an}}\right] - \exp\left[\frac{-\eta}{B_{a,b}^{cat}}\right]\right\} \cong$$

$$\left\{k_{a,b}\cdot[O_2]\right\}\cdot\left\{\frac{B_{a,b}^{an}\cdot B_{a,b}^{cat}}{B_{a,b}^{an}+B_{a,b}^{cat}}\cdot\left(\phi_c-\phi_{el}\right)\right\}$$

where $i_{a,b}^{(0)}$ are the exchange current densities, $B_{a,b}^{an}$ and $B_{a,b}^{cat}$ are the anodic and cathodic Tafel slopes respectively and $k_{a,b}$ are kinetic constants.

Mass transport of $O_2$ in the agglomerate cathode is described by Fick's law:

$$-D_{eff}\cdot\nabla^2[O_2] + \frac{i_{e,c}}{2F} = 0$$

$$i_{e,c} = i_{e,c}^{(0)}\left([O_2]\right)\cdot\left\{\exp\left[\frac{\eta}{B_{e,c}^{an}}\right] - \exp\left[\frac{-\eta}{B_{e,c}^{cat}}\right]\right\} \cong$$

$$\left\{k_{e,c}\cdot[O_2]\right\}\cdot\left\{\frac{B_{e,c}^{an}\cdot B_{c,c}^{cat}}{B_{e,c}^{an}+B_{e,c}^{cat}}\cdot\left(\phi_c-\phi_{el}\right)\right\}$$

where the subscripts *e, c* denote electronic conduction in the cathode and $D_{eff}$ is the effective diffusion coefficient of $O_2$.

In both the current and the mass balances, in the cathode domain, the porous structure is

accounted for by introducing effective transport parameters.

The first step of this analysis was to select suitable changes of the input variables (cell voltage and $O_2$ concentration) and material parameters - listed below -, accounting for the impact of the corrosion of metallic current collectors on the performance of the porous cathode. In fact, release of transition metal corrosion products at the current collector/porous cathode interface is likely to clog the pore structure and contaminate the catalyst surface, resulting in: (i) decrease of $O_2$ effective mass transport, (ii) reduced ionic conductivity and (iii) lower values of the kinetic constants.

The second step was to introduce in the governing equations of the model a steady-state thermal equation, defined in the domanis α and β (Fig. 2 B):

$$K_b\left(T_b\right)\cdot\nabla^2 T_b + Q_b\left(i_{e,b}+i_{I,b}\right)=0$$

where $Q_b\left(i_{e,b}+i_{I,b}\right)$ is the source function in domain *b*; $i_{e,b}$ and $i_{I,b}$ are the local current densities. The thermal conductivity of molten salts $K_{el}\left(T_{el}\right)$ as a function of temperature was interpolated from a range of experimental measurements from the literature [6]:

$$K_{el}\left(T_{el}\right)=$$

$$0.8833-1.5365\cdot 10^{14}\cdot\exp\left[-\frac{T_{el}}{24.172}\right]$$

The thermal conductivity of the current collector bulk is equated to the typical value of stainless steel 11.5 W $m^{-1}$ $K^{-1}$.

## 3. Use of COMSOL Multiphysics

We start by considering the demo MCFC [7] available in the Chemical Engineering module of Comsol Multiphysics© v.3.4.

The boundary conditions associated to the thermal equation are illustrated in Fig. 3 that shows the two domains considered in the model.

In particular, for the thermal flow condition (6 in Fig.3) we considered the heat transport coefficient present in the model material library as appropriate.

Furthermore, we expressed electrode conductivity $k_{cat}$, ionic conductivity in the electrode $k_{ion}$ and ionic conductivity in the free electrolyte $k_{el\_free}$ as functions of temperature and obtain their dependency interpolating literature experimental results [8]

$$k_{cat}\left(T\right)=-8.928+0.0331\cdot T$$
$$k_{ion}\left(T\right)=26.29-0.02306\cdot T$$
$$k_{e\_free}\left(T\right)=749.1-0.6575\cdot T$$

The cathodic polarization curves corresponding to the standard operative conditions (0.15 V, $O_2$ concentration 1.98 [mol·$m^{-3}$] that can be regarded as a reference condition) without and with coupled thermal equations are plotted in Fig.4.

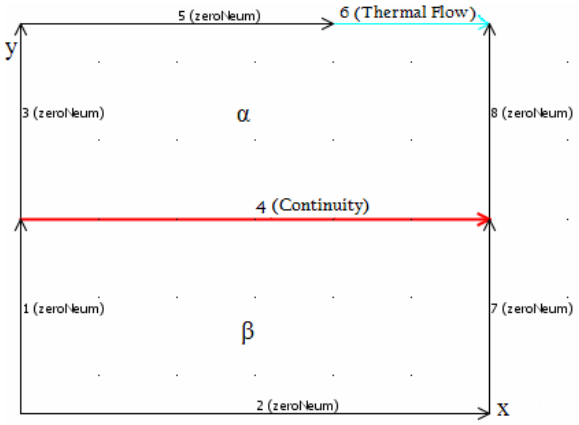


**Figure 3.** Boundary conditions for the thermal equation

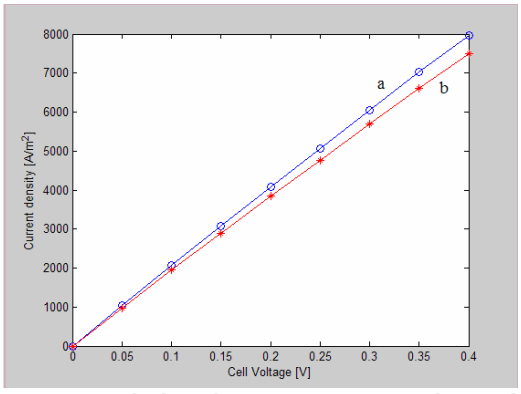


**Figure 4.** Cathodic polarization curves (a) without and (b) with coupled thermal equation.

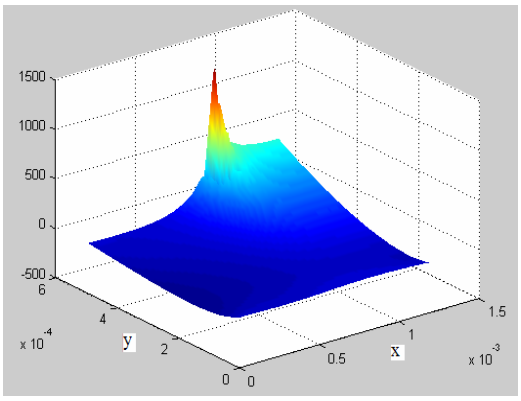


**Figure 5**. Difference $\Delta i$ between module c.d. values in temperature independent and dependent models.

Furthermore, Fig. 5 shows the differences $\Delta i$ between current density values in these two cases:

$$\Delta i = \left(\left|i_{e,c}\left(T = 650°C\right)\right| + \left|i_{I,c}\left(T = 650°C\right)\right|\right) - \left(\left|i_{e,c}\left(T\right)\right| + \left|i_{I,c}\left(T\right)\right|\right)$$

Our computations show that the introduction of the therrmal equation affects the modulus of the current density in two chief ways: (i) near the current collector - owing to the increase of temperature - $\Delta i$ is positive because the decrease of ion transport conductivity prevails; (ii) far from the current collector $\Delta i$ is negative because the electronic conductivity increases.

## 4. Results

Fig. 6 shows a typical distribution of the vertical component of the current density (c.d.) in the cathode domain, computed at the reference condition.

Fig. 7 shows the computed polarization curves, corresponding to three different $[O_2]$ values: (a) 1.98 (the standard condition), (b) 0.2 and (c) 0.02 mol $m^{-3}$. The polarization curve for the standard composition shows an almost straight line with no bending even at high current density, while lower oxygen contents result in a limiting current behavior.

The distributions of temperature (coloured surface) and c. d. (height), corresponding to the model including the thermal equation, are shown in Fig. 8.

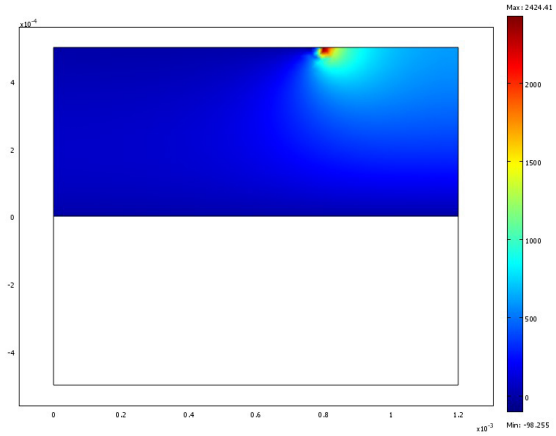


**Figure 6**. A typical distribution of the vertical c.d. component at 0.15 V.

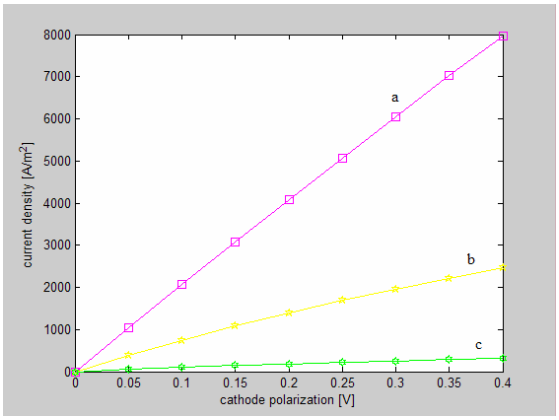


**Figure 7**.I-V characteristics for $O_2$ concentrations equal to (a) 1.98, (b) 0.2, (c) 0.02 mol $m^{-3}$.

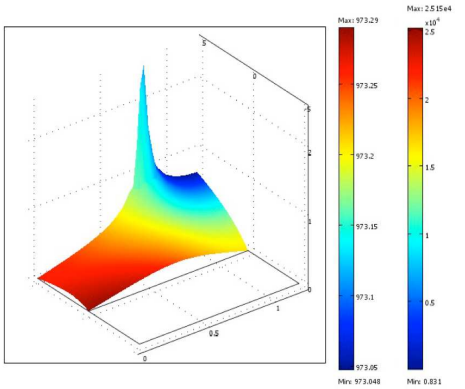

**Figure 8** A typical distribution of the temperature (surface) and of the module c.d. (height) (0.30 V and $[O_2]$ =1.98 mol $m^{-3}$).

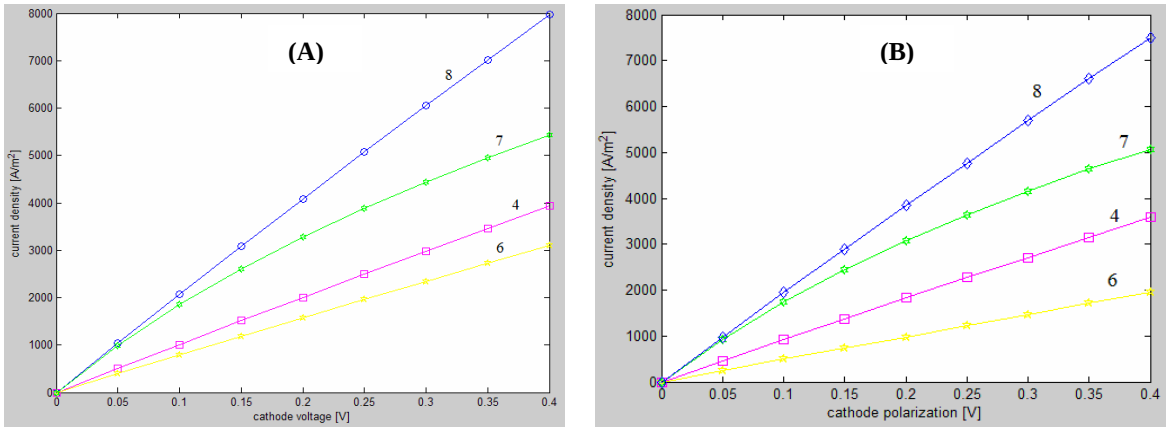


**Figure 9**. I-V curves for typical DOE cases: (A) for the temperature independent condition and (B) after introduction of the thermal equation.

## 4. 1 The DOE analysis

Design of experiments (DOE) is a useful and straightforward tool to determinate the extent to which a specific factor affects a process [9]. The focus will be on two level factorial design with 8 runs, where each input variable is varied at high (+) and low (-) levels.

We considered as main parameters involved in corrosion: (i) the effective conductivity related to the electrolyte in cathode ($k_{ion}$); (ii) the effective exchange current density ($k_{cat}$) and (iii) the effective oxygen diffusion coefficient ($D_{eff}$). We carried out a two level DOE analysis considering the reference parameters values ($k_{ion}$ = 5 S/m, $k_{cat} = 6.7 \cdot 10^{7}$ S/mol, $D_{eff} = 2.8 \cdot 10^{-5} m^2/s$) as the upper level and these reference values divided by a factor of 10 as the lower level.

Likewise, the DOE analysis in the temperature-dependent case, was carried out by defining the high and low levels of the three temperature-dependent quantities $\chi_i(T)$ (with *i=1,2*,3), terms of the high and low levels of the corresponding fit parameters $p_j$ (with *j=1,2*,3 or *1,2*).

$$high\left[\chi_i(T)\right] = \chi_i\left(T; high\left(p_j\right)\right)$$

$$low\left[\chi_i(T)\right] = \chi_i\left(T; low\left(p_j\right)\right)$$

The experimental matrix, common to each set of runs, is reported in Table 1 and the results of the DOE analysis are given in Table 2.

A selection of representative I-V curves are shown in Fig. 9 (the numbers denoting the curves correspond to the labels of the experimental matrix) .

| Esperiment | $D_{eff}$ | $k_{cat}$ | $k_{ion}$ |
|---|---|---|---|
| 1 | - | - | - |
| 2 | − | - | - |
| 3 | - | + | - |
| 4 | − | + | - |
| 5 | - | - | + |
| 6 | − | - | + |
| 7 | - | + | + |
| 8 | − | + | + |

**Table 1**. Experimental matrix of DOE

## 7. Conclusions

From the COMSOL runs described above and from our DOE analysis, we can conclude that the model exhibits the highest sensitivity to corrosion-induced material parameter changes for catalyst poisoning, followed by single-factor effects relating to pore clogging, the higher relative impact corresponding to ion transport.

Considering the temperature influence on the process, we can say that no changes occur in the order of the critical parameters, but the relative importance of catalyst poisoning is further stressed.

**(A)**

| | |
|---|---|
| $k_{cat}$ | 100 |
| $k_{ion}$ | 80 |
| $D_{eff}$ | 41 |
| $k_{cat} \cdot k_{ion}$ | 37 |
| $D_{eff} \cdot k_{cat}$ | 26 |
| $D_{eff} \cdot k_{ion}$ | 16 |
| $D_{eff} \cdot k_{cat} \cdot k_{ion}$ | 8 |

**(B)**

| | |
|---|---|
| $k_{cat}$ | 100 |
| $k_{ion}$ | 62 |
| $D_{eff}$ | 31 |
| $k_{cat} \cdot k_{ion}$ | 40 |
| $D_{eff} \cdot k_{cat}$ | 26 |
| $D_{eff} \cdot k_{ion}$ | 13 |
| $D_{eff} \cdot k_{cat} \cdot k_{ion}$ | 10 |

**Table 2.** Results of DOE analysis: (A) without and (B) with the effect of thermal equation.

## 8. References


1. G. Durante, S. Vegni, P. Capobianco, F. Galgovici, High temperature of metallic materials in molten carbonate fuel cells environment, *Journal of Power Sources*, 152, 204, (2005).
2. X. Songbo, Z. Yongda, H. Xing, Z. Bangna, Y. Zhongxing, *Journal of Power Sources*, 103, 230-236, (2006).
3. B. Bozzini, D. Lacitignola, I. Sgura. *Journal of Phys*: Conf. Series 96 (2008) 012051.
4. E. Fontes, C. Lagergren, G. Lindbergh, D. Simonsson, Influence of gas phase mass transfer limitations on molten carbonate fuel cell cathodes, *Journal of Applied Electrochemistry*, 27, 1149, (1997).
5. E. Fontes, M. Fontes, D. Simonsson, A heterogeneous model for the MCFC cathode, *Electrochimica Acta* 40, 1641, (1995).
6. X.Zhang, M.Fujii, Simultaneous measurements of the thermal conductivity and thermal diffusivity of molten salts with transient Short-Hot-Wire method, *International Journal of Thermo physics*, 21, 79 (2000)
7. COMSOL MULTIPHYSICS v.3.4 Chemical Engineering Module, Model Library, p. 541 (2007).
8. M.Yoshikawa, A. Bodén, M. Sparr, G. Lindbergh, Experimental determination of effective surface area and conductivities in the porous anode of molten carbonate fuel cell, *Journal of Power Sources*, 158, 97 (2006)
9. Box, Hunter and Hunter, *Statistics for Experimenters*, John Wiley & Sons (1978).